AR08

Pipeline Defects' Length Estimation Using MFL Signals

Taewook Kim[1], Doo-Hyun Choi[1]*, and Sung-Ho Jo[2]

[1]School of Electrical Engineering and Computer Science, Kyungpook National Univ., Daegu, South Korea
[2]Kogas R&D Division, Ansan, Kyunggido, South Korea

* Corresponding author: Doo-Hyun Choi, e-mail: dhc@iisl.knu.ac.kr

Nondestructive testing and evaluation techniques for underground pipeline inspection include signal processing using MFL (Magnetic flux leakage) sensors, eddy current sensors, ultrasonic sensors, cameras, etc. Among them, MFL based techniques are widely used for underground pipeline inspection. MFL signal is gathered using MFL PIG (pipeline inspection gauge) which is equipped with several permanent magnets, hall sensors and a data acquisition system. This paper presents two length estimation methods using the MFL signal. One is based on thresholding of axial MFL signal and the other is based on thresholding of radial MFL signal. First of all, nine artificial defects whose geometric information (length, width, depth, and surface angle) is known are carved into a sample pipeline. Fig. 1 overlays the two thresholding results and Table 1 summarizes actual lengths and the estimation results for different thresholds using axial and radial signals.

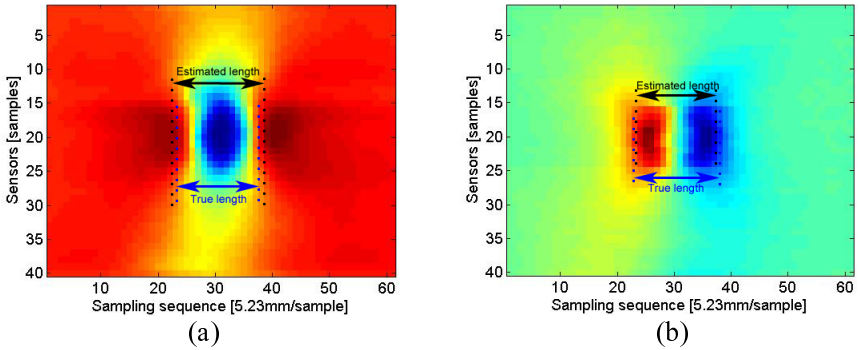

Fig. 1. Length estimation of Defect No. 6 by thresholding for (a) axial MFL signal, (b) radial MFL signal.

Table 1. Estimated lengths for different thresholds.

Defect No.	Actual Length [mm]	Threshold for Axial MFL Signal			Threshold for Radial MFL Signal		
		0.1	0.2	0.3	0.8	0.9	1
1	35	41.84	36.61	36.61	47.07	36.61	36.61
2	34	47.07	41.84	36.61	47.07	41.84	36.61
3	35	52.3	41.84	36.61	41.84	41.84	31.38
4	70	78.45	67.99	62.76	73.22	73.22	62.76
5	70	78.45	67.99	62.76	83.68	73.22	62.76
6	70	78.45	73.22	62.76	78.45	67.99	62.76
7	105	109.83	99.37	94.14	104.6	104.6	94.14
8	105	109.83	104.6	94.14	109.83	104.6	94.14
9	105	109.83	94.14	94.14	109.83	99.37	88.91
Average Error		8.37	**3.34**	6.59	7.33	**4.38**	7.44

AR09

Nanostructuring Paramagnetic Molecules at Metal Surfaces as a Template for ESN-STM

Paolo Messina*, Frank Y. Fradin, John J. L. Morton, Andrea Caneschi, Matteo Mannini, and Lorenzo Sorace

Material Science Division, Argonne National Laboratory, Argonne US
Materials Department, Clarendon Laboratory, Oxford University, UK
Laboratory for Molecular Magnetism, Department of Chemistry, University of Florence & INSTM R.U., Florence, Italy

Both the measurement of spin dynamics at the single molecular level1-3 and the exploration of paradigms to implement quantum computing at the nanoscale require a precise spatial control on the position of the spin. Unpaired electron spins in organic molecules are interesting candidates for this purpose: the low spin orbit coupling of the unpaired electron in an organic molecule and the synthetic flexibility in adding molecular moieties, make these molecules appealing for surface constrained nanostructuring. In this work we present three different approaches to the nanostructuring of paramagnetic organic molecules at the surface. We use the Au(111) surface for the three methods.

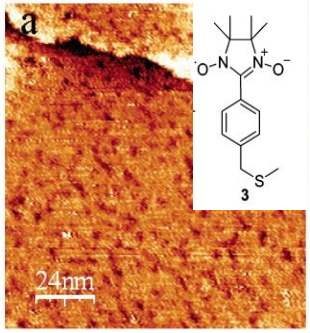

STM image of ordered arrays of the nitronyl nitroxide (NIT-PhR) derivative shown in the inset.

In the first approach a nitronyl nitroxide radical (NIT) moiety is functionalized with three different linking groups (Ph-R; with R = CH_2SCH_3, SCH_3, $PhSCH_3$) including in all cases a sulfur atom[4] promoting the interaction with gold. Depending on the tail structure self assembling of ordered monolayers of spins are observed. In this way a commensurate lattice of spin centers is created. Electron Spin Resonance (ESR) measurements are obtained from these monolayers. These measurements show that the monolayers preserve the molecular paramagnetism, in addition they also provide evidence that the molecules are subject to slow movements around their axis.

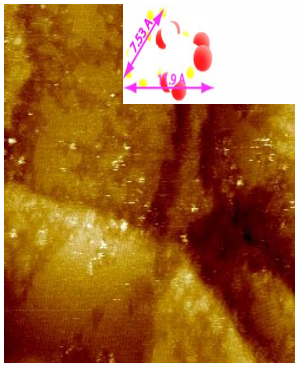

STM image of ordered arrays of 1-10 phenantroline. The white protrusions are DPPH single molecules or dimers.

In the second approach paramagnetic molecules of DPPH are embedded into a 2D-ordered diamagnetic molecular matrix[5]. This approach is particularly useful to provide a test sample for Scanning Tunneling Microscope (STM) single molecular spectroscopy at room temperature at the solid air-interface. Ordered arrays of the molecule 1-10 phenantroline are created on Au(111) by dipping method followed by sample annealing to 80 °C. Specifically a mixture containing the paramagnetic molecule DPPH and the 1-10-phenantroline is used to produce the nanostructure.

ESR measurements provides insights on the thermal resilience of the DPPH molecules. The STM data are interpreted making use of ENDOR and FT-ESR measurements obtained from solid and liquid dilute solutions of DPPH.

In the third approach we make use of a Nitroxyl Nitroxydes (NIT) moiety bringing an anthracene tail. This tail allows the formation of ordered monolayers of NIT-anthracene molecules on the Au(111) surface. ESR spectra are obtained from the monolayer surface showing that the paramagnetism of the NIT moiety is preserved at the contact with the surface. Electron Nuclear Double Resonance (ENDOR) and Electron Spin Envelope Echo Measurement(ESEEM) measurements from dilute solid and liquid solution are also presented. The ENDOR measurements provide the relaxation time for the N nuclei, which assists the interpretation of single molecule spectroscopy measurements. STM measurements from diamagnetic anthracene films intercalated with NIT-anthracene molecules will be also presented.

REFERENCES

[1] Messina, P.; Mannini, M.; Caneschi, A.; Gatteschi, D.; Sorace, L.; Sigalotti, P.; Sandrin, C.; Prato, S.; Pittana, P.; Manassen, Y., Spin noise fluctuations from paramagnetic molecular adsorbates on surfaces. Journal of Applied Physics 2007, 101, (5), -.

[2] Manassen, Y.; Komeda, Distribution of frequencies of a single precessing spin detected by ESR-STM. Applied Physics Letters 2008, accepted.

[3] Mannini, M.; Messina, P.; Sorace, L.; Gorini, L.; Fabrizioli, M.; Caneschi, A.; Manassen, Y.; Sigalotti, P.; Pittana, P.; Gatteschi, D., Addressing individual paramagnetic molecules through ESN-STM. Inorganica Chimica Acta 2007, 360, (13), 3837-3842.

[4] Mannini, M.; Sorace, L.; Gorini, L.; Piras, F. M.; Caneschi, A.; Magnani, A.; Menichetti, S.; Gatteschi, D., Self-assembled organic radicals on Au(111) surfaces: A combined ToF-SIMS, STM, and ESR study. Langmuir 2007, 23, (5), 2389-2397.

[5] Messina, P.; Fradin, F., Imaging Single Spin Probes Embedded in a conductive Diamagnetic Layer. 2008, in preparation.

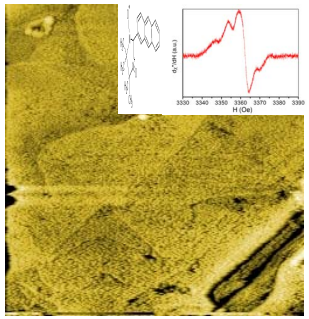

STM image of ordered arrays of NIT-anthracene phenantroline. The inset shows the NIT-anthracene molecular structure and the ESR image obtained from.

AR10

Ultrafast Phenomena of Charge-ordering Phase in $La_{1/4}Pr_{3/8}Ca_{3/8}MnO_3$

Kyeong-Jin Jang[1], Jongseok Lim[1], Jaewook Ahn[1]*, Jihee Kim[2], Ki-Ju Yi[2], and Jai Seok Ahn[3]

[1]Department of Physics, KAIST, Daejeon 305-701, Korea
[2]Department of Physics, Chungnam National University, Daejeon 305-764, Korea
[3]Department of Physics and RCDAMP, Pusan National University, Pusan 305-764, Korea

*Corresponding author: Jaewook Ahn, e-mail: jwahn@kaist.ac.kr

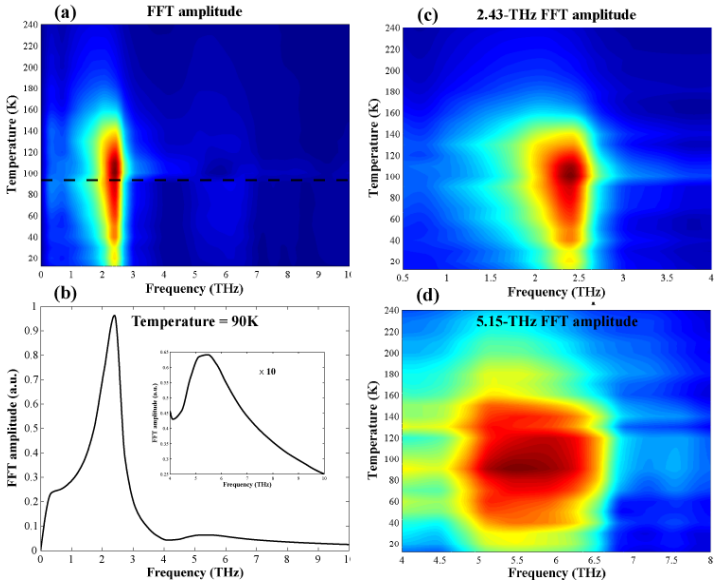

Fig. 1. The gereration of coherent optical phonons in $La_{1/4}Pr_{3/8}Ca_{3/8}MnO_3$ (a) Fourier- transform of coherent oscillations. (b) Two modes of coherent optical phonons appearing at 90 K (charge-ordering phase). (c), (d) Temperature dependence of optical phonon spectrum of 2.43 THz and 5.15- THz, respectively.

We have used 1.5 eV pump-and-probe spectroscopy to investigate the optical phonon modes of a phase-separated manganite, $La_{1/4}Pr_{3/8}Ca_{3/8}MnO_3$(LPCMO). LPCMO has the mixed-phase of ferromagnetic metal(FM) and charge-ordering insulator(CO) coexisting as submicrometer-sized domains[1]. Related with the domain size dynamics of the CO phase, we have obtained several temperature dependent phenomena such as coherent optical phonon generations (two modes), an acoustic phonon generation, and multiple time-scale relaxations involving electron, lattice, and spin carriers. Fig. 1 shows the temperature dependence of coherent optical phonon generations of 2.43- and 5.15-THz phonons. These optical phonon modes appear in conjunction with the charge-ordering phase below TCO. However, below TC (=110 K), the amplitudes of these phonons begin to fall with the increase of FM domain fraction [2]. These scaling behaviors indicate that the optical phonons are related with the CO phase only in these structural mixed-phases of LPCMO.

REFERENCES

[1] M. Uehara et al., Nature 399, 560 (1999).
[2] K.H. Kim et al., Phys. Rev. Lett. 84, 2961 (2000).